JOURNAL OF GEOPHYSICAL RESEARCH, VOL. 115, E04009, doi:10.1029/2009JE003481, 2010

A fundamental parameters approach to calibration of the Mars Exploration Rover Alpha Particle X-ray Spectrometer: 2. Analysis of unknown samples

J. L. Campbell,[1] S. M. Andrushenko,[1] S. M. Taylor,[1,2] and J. A. Maxwell[1]

Received 29 July 2009; revised 20 November 2009; accepted 14 December 2009; published 28 April 2010.

[1] Our fundamental parameters method was recently applied to results from geochemical reference materials to provide a new calibration of the laboratory Alpha Particle X-ray Spectrometer (APXS) instrument from the Mars Exploration Rovers mission. The method is now extended to provide an iterative approach for the treatment of unknown samples, based upon that initial calibration. It is tested by regarding small subsets of the reference materials and other materials as unknown samples; agreement of derived element concentrations with suppliers' recommended values is good with the exception of certain igneous rock types. In these exceptions, the deviations can be explained via the location of the elements concerned in minority or accessory mineral phases, and different calibration schemes can be developed empirically for specific rock types which are defined via a TAS diagram. The necessary reliance upon an iterative approach in normalizing the sum of oxide concentrations to 100% is investigated. It turns out that this can cause significant errors in derived element concentrations when a significant amount of mineralogically bound water (H_2O+) is present, but our method has been extended to enable determination of this H_2O+ concentration under known geometry. Various implications for calibration of the new APXS selected for the Mars Science Laboratory are discussed.

Citation: Campbell, J. L., S. M. Andrushenko, S. M. Taylor, and J. A. Maxwell (2010), A fundamental parameters approach to calibration of the Mars Exploration Rover Alpha Particle X-ray Spectrometer: 2. Analysis of unknown samples, *J. Geophys. Res.*, *115*, E04009, doi:10.1029/2009JE003481.

1. Introduction

[2] In a recent paper [*Campbell et al.*, 2009] bearing the same title as this one, we introduced the basis of a new approach to the extraction of element concentrations from spectra recorded by Alpha Particle X-ray Spectrometers (APXS) of the type used on the Mars Exploration Rovers (MER). The data which we used to test our method were the original MER APXS calibration spectra, taken on a laboratory instrument of the same design as the flight instruments [*Gellert et al.*, 2006]. The samples used to generate these spectra were a suite of widely varied geochemical reference materials (GRM) obtained from several suppliers, together with a number of pure elements and simple chemical compounds. All the GRMs and the majority of other standards were in powder form, sieved through a mesh to exclude particles over 75 μm in diameter. In this paper we extend our new approach to the point where it appears ready for application to analysis of data from unknown samples. In effect, this is a continuation of the previous paper, which we shall refer to as Part I. We shall minimize repetition of the material of Part I, except where it is crucial to arguments being made here. Within the overall objective of testing the new approach, there are two major points of interest. The first of these is the possibility that the APXS calibration might differ for GRMs that have different mineralogy. The second is the influence of mineralogically bound water on the analytical accuracy. Our results will influence the calibration of the APXS that is to be used on the upcoming NASA Mars Science Laboratory mission.

[3] Our approach to the deduction of element concentrations from the APXS spectra differs from that employed by the MER team [*Gellert et al.*, 2006]. They used a peak-fitting program to provide the areas of the Kα (or Lα) X-ray peak for each element in each reference material. A matrix correction was then applied, separately from the peak-fitting process, to account for X-ray attenuation effects within each GRM. For a given element, this matrix correction was a linear combination of an XRF matrix correction and no correction, with a weighting factor determining the ratio of these two contributions. For each element, an iterative optimization procedure was applied to determine the best values of this weighting parameter and of a "response" parameter, the latter being defined as the ratio between the element's X-ray

[1] Guelph-Waterloo Physics Institute, University of Guelph, Guelph, Ontario, Canada.
[2] Department of Atmospheric and Oceanic Sciences, McGill University, Montreal, Quebec, Canada.

0148-0227/10/2009JE003481

counts and concentration in the absence of matrix effects. The ratio between the attenuation coefficient in the GRM for the characteristic X-ray of the element in question and the mean value of this quantity across the suite of GRMs was a necessary third parameter used in this process. After application of the matrix correction, the resulting element concentrations were converted by stoichiometry to oxide concentrations and normalized to a total concentration of 100 wt %. The resulting calibration was then applied to the results from an unknown sample. Rather than determining separate response and weighting factors for each element, our approach is to determine a single calibration factor for the instrument, with both XRF and PIXE matrix effects incorporated rigorously within the spectrum fitting code. The results for each element can then be assessed in turn in order to determine if they deviate from expectation. This helps us to understand the causes of any such deviations, and to develop element-specific corrections which might depend upon the various rock types within the suite of GRMs. This approach demands the fullest possible understanding both of the X-ray physics that governs the various interactions within the sample and of the properties of the X-ray detector. We shall not repeat here the extensive detail on this method that we provided earlier; however, it is necessary to give a brief outline as a foundation for the further developments that are our main subject here.

[4] In Part I, we showed that the observed yield $Y(Z)$ of a specific characteristic X-ray of a given element (atomic number Z, concentration C_Z) in an APXS measurement of duration T seconds is

$$Y(Z) = H\, C_Z\, T\, k(Z)\left[Y_{1,\mathrm{PIXE}}(Z,M) + \Sigma\, Y_{1,\mathrm{XRF}}(Z,M)\right] t_Z\, \varepsilon_Z \quad (1)$$

The first term represents X-rays from the PIXE (particle-induced X-ray emission) process arising from the alpha particles emitted by the APXS excitation source (^{244}Cm). The second term represents X-rays from the XRF (X-ray fluorescence) process arising from plutonium L X-rays from the source. In either case $Y_1(Z,M)$ is the computed theoretical X-ray yield from element Z per unit concentration within a defined matrix M, per steradian of solid angle, per ion or photon. The summation in the XRF case reflects the existence of approximately 20 L X-ray lines, each having a unique energy, emitted by ^{244}Cm. Computation of the quantity $Yi(Z,M)$, which rigorously describes the matrix effects, demands an extensive atomic physics database which includes charged particle ionization cross sections, photoionization cross sections, ion stopping powers and X-ray attenuation coefficients. The X-ray transmission fraction through any material interposed between the detector and the sample surface is t_Z. The intrinsic efficiency of the detector is ε_Z. In the vicinity of the iron K X-rays ε_Z is close to 1.0; at low X-ray energies it decreases markedly due to the attenuating effects of the beryllium window and the nitrogen filling; at high energies it decreases because the thickness of the silicon detection wafer is insufficient to provide complete absorption. While the manufacturer provides values for the thicknesses of the wafer and the attenuators, these should not be assumed to be 100% accurate. The manufacturer does not provide numerical detail on a layer of incomplete charge collection (ICC), which would depress the efficiency for those X-rays (P, S, Cl) that are absorbed preferentially very close to the detector surface, but such an ICC effect is described in the literature [*Eggert et al.*, 2006]. Insight into these various quantities can be developed through APXS analyses of pure element and simple chemical compound standards.

[5] The single instrumental calibration factor is H, and it has to be determined in the calibration exercise. As shown in Part I, this factor accounts for the instrument geometry and the source activity. If the physics database is accurate and the detector parameters and properties are accurately known, measurements on reference materials should, in principle, provide an H value that is independent of Z or of X-ray energy. In practice small Z dependences have been observed during development of the PIXE analysis technique [*Campbell et al.*, 1993], often necessitating insertion of an experimentally determined corrective function $k(Z)$, having values slightly different from a default value of 1.0. Among the objectives of Part I were to ascertain if such a $k(Z)$ function was required for the APXS and to understand the underlying reasons for this. We reiterate that the reasons could lie in the database, the detector description and in geochemical effects, all of which were discussed previously.

2. Prior Results

[6] In Part I of this work, we used our new computer code GUAPX to fit the geological reference material spectra that were recorded in the MER APXS calibration exercise by *Gellert et al.* [2006] We specifically assumed the suppliers' elemental concentrations C_Z in order to compute the matrix terms Y_1 which are required in equation (1). We refer to this method as the fixed matrix approach. We first determined the system H parameter to be the particular value that provided agreement with the suppliers' concentrations for the abundant element silicon in the GRMs; this result agreed at the 1% level with the value obtained from standards of SiO and SiO_2. We then examined the ratio R between the GUAPX concentration and the supplier's recommended concentration for all other detectable elements in all the GRMs. Ideally, the weighted mean R_{wm} for a given element across all the GRMs would be unity.

[7] Before we discuss these GRM results, which are in Table 1, we must recall that in two regions of atomic number ($Z \leq 13$ and $15 \leq Z \leq 17$) we cannot expect an R value of 1.0, because of our deliberate omission from the detector model of an incomplete charge collection layer at the crystal surface. Our analyses in Part I of the spectra taken by *Gellert et al.* [2006] from standards of pure elements and simple compounds strongly suggested the presence of such a layer, but were insufficient to enable development of a model for it within our overall detector description. The most significant effect of this ICC layer would be a sudden drop in detector efficiency and therefore in R value for elements such as phosphorus, sulfur and chlorine whose K X-ray energies lie just above the silicon K absorption edge, resulting in their strong absorption within the ICC layer. In Table 1 we observe this effect occurring for the phosphorus K X-rays, after which the R value quickly recovers toward 1.0 as Z increases. Such an ICC layer would also cause a similar falloff at very low Z values, and such behavior is also seen in Table 1. However, at such low X-ray energies it is not possible to distinguish the ICC effect from

Table 1. *R* Values and Uncertainty Estimates From Part I for Simple Element and Compound Standards and for the GRMs[a]

			Geochemical Reference Materials			
Z	Element	Simple Standards *R*(fit)	R_{wm}	SD	*EEM*	Comments
11	Na	0.88	0.99	0.12	0.02	Three distinct GRM subgroups apparent
12	Mg	0.96	0.90	0.12	0.02	
13	Al	0.99	1.047	0.10	0.01	Three distinct GRM subgroups apparent
14	Si	1.00	1.00	0.033	0.006	
15	P	0.87	1.23	0.26	0.05	Two distinct GRM subgroups apparent
16	S	0.94	0.97	0.28	0.07	
17	Cl	0.96	1.19	0.23	0.08	GRM MAG-1 differs from others
19	K	0.99	1.025	0.047	0.013	
20	Ca	1.00	1.043	0.038	0.013	
22	Ti	1.00	0.926	0.12	0.02	
24	Cr	1.01	1.10	0.1	0.1	
25	Mn	1.00	1.034	0.094	0.048	
26	Fe	1.00	0.984	0.034	0.008	
30	Zn	1.00	0.983	0.12	0.04	

[a]For the GRM suite, R_{wm} is the error-weighted mean, SD is the standard deviation, and *EEM* is the estimated (standard) error of the mean. For the simple standards, an empirical fit to the measured *R* values was used.

changes in the predicted "window attenuation" due to slight variations from the manufacturer's quoted thicknesses for the beryllium window and the nitrogen column. Sample surface roughness effects would also increase rapidly with decreasing atomic number.

[8] The R_{wm} values found for the GRM suite should be judged by whether or not they agree with the values from the simple elements and chemical compound standards; in most cases this implies an expected R_{wm} value of 1.0, but not in the cases of phosphorus, sulfur and chlorine. With exceptions that we will discuss immediately, there is good agreement for most major and minor elements, and this persists for the trace elements (with larger uncertainties which reflect both statistical error and suppliers' uncertainty estimates).

[9] For phosphorus, the GRM data fall into two distinct groups: results for the small group of homogeneous minerals agree well with the *R* values of the simple phosphorus compounds, while the values for igneous rocks are much larger, suggestive of an inhomogeneous distribution of phosphorus in the latter. This is not surprising since phosphorus is often present in apatite phases rather than uniformly distributed within the rock. The chlorine case resembles that of phosphorus, although with large attached uncertainties, suggesting the same combination of explanations. It is noteworthy, though, that the sediment MAG-1, which has by far the largest concentration of chlorine, has $R = 0.86$ while the other fourteen GRMs (mostly igneous rocks) have $R_{wm} = 1.19$. The uniformly low R_{wm} for magnesium in the GRMs, which is not dissimilar to the value for the simple chemical standards, is seen as a database or sample surface imperfection issue for low-energy X-rays.

[10] The observed dependence of the sodium and aluminum *R* values in igneous rocks upon SiO_2 content led us to the idea that "subcalibrations" might be developed for different rock types as defined by a total alkali versus silicates diagram [*LeMaitre et al.*, 2002], and we therefore used the diagram of Figure 1 (supplied by P. King, private communication, 2008) to separate such GRMs into basalt, andesite and rhyolite classes for calibration purposes. In the rest of this paper the terms basalt, andesite and rhyolite will reflect the position of the pertinent igneous rock GRM in the TAS scheme. For both sodium and aluminum, three distinct behaviors were visible in the data, with different weighted mean *R* values for basalts (whose R_{wm} values were typically about 1.2), andesites, and rhyolites. The sodium mean *R* values all exceeded the result from a simple NaCl standard; the low *R* value for the latter may reflect an imperfectly smooth sample surface or database issues at very low atomic number. The raised values for aluminum and sodium in these igneous GRMs were discussed in extensive detail in Part I and attributed through semiquantitative arguments to mineral phase heterogeneity typical of the pertinent rock class. Since the sample is assumed to be homogenous, the matrix term in equation (1) is dominated by the composition of the majority phase (e.g., olivine and pyroxene in basalt). But in basalts and andesites, sodium and aluminum tend to occur in the minority phases such as feldspar. The helium ions only penetrate a few microns into the sample; since they interact with only such a small portion of the sample, this portion is likely to be composed of only one phase. It follows that the average matrix term cannot be accurate for elements which occur predominantly within minority or accessory phases. Further evidence to support this explanation will be presented in section 7.

[11] In Part I, we attributed the low-lying R_{wm} value for titanium in the GRMs to our treatment of the overlapping escape peak of the intense iron X-ray line. Based on calculations with the escape intensity model of *Campbell et al.* [1998], we now believe this attribution to be incorrect. Since titanium in igneous rocks occurs in the accessory titanite phase, the effect is probably another example of an incorrect matrix term, analogous to the sodium and aluminum examples discussed above.

[12] Overall, with explanations offered for the special cases, the results of Part I support our contention that the APXS can be described by a single instrumental constant provided that the database is accurate and the detector is well understood. Nevertheless, there is important further work to do on both these aspects. In addition, the ideas on the effects of mineral phase heterogeneity need further development and testing, both here and in the much more extensive calibration exercise that is underway for the Mars Science Laboratory APXS. Despite these caveats, it is encouraging that for both rhyolites and homogeneous materials (simple chemical compounds and nearly pure

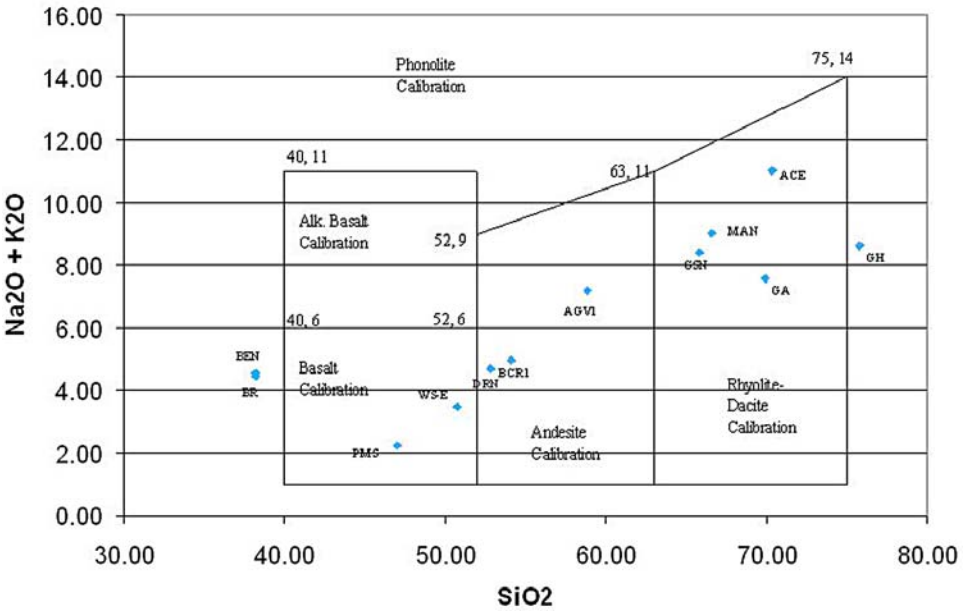

Figure 1. Total alkali versus silicate content diagram, including the specific standard rocks used in this work and showing regions of potentially different calibration.

mineral GRMs), a single *H* value gives excellent concentration values; this confirms the validity of the model used, including the database for X-ray excitation and transmission within the sample.

3. Methodology for Analysis of Unknown Samples

[13] In the real situation on Mars, the analytical challenge is much more difficult than in the rather straightforward case of a terrestrial analysis of known reference materials. There is no a priori knowledge of the samples, and the exact distance to the detector is not known. The fixed matrix (FM) approach is obviously inapplicable. The only possibility is an iterative solution, referred to here as the iterative matrix (IM) approach. GUAPX commences with a preliminary fit of the spectrum in which no matrix corrections are done, for the obvious reason that no concentrations are known. The resulting peak areas are converted via equation (1) and the *H* value (known from prior calibration on Earth) into element concentrations, and thence into oxide concentrations via assumed stoichiometry. The total concentration is then normalized to 100%; this step provides a first estimate of the sample matrix. This estimate is used to generate the matrix corrections during the second iteration, which yields a new set of concentrations. The process is iterated, with the goodness-of-fit (reduced chi-square) reoptimized within each iteration, until the matrix concentrations are consistent. The 100% closure condition renders the absolute value of *H* redundant; the program determines a new, effective *H* value consistent with the normalization. If these two values differ by more than 1%, their ratio (H_{corr}) is provided in the GUAPX output as a diagnostic that the geometry or some other factor has changed relative to expectations. However, the $k(Z)$ function is not redundant.

[14] We note in passing that the approach of *Gellert et al.* [2006] was also based upon the 100% closure rule. It is a standard approach in X-ray emission analysis of geological materials [*Potts*, 1987].

[15] An iterative matrix approach becomes problematic for samples that contain additional "X-ray invisible" components beyond the oxygen that is bound via stoichiometry to the cations. Such components include carbon, carbon dioxide, boron and lithium oxides, and mineralogically bound water (denoted H_2O+). These components were not an issue in Part I of this work, because there the fixed matrix was constructed to include their known amounts, and the matrix calculations were therefore rigorous. But now, in the iterative approach, if significant invisible components are present in an unknown sample, one must expect the generated matrix to be incorrect. This outcome may be detectable in the GUAPX output through the value of H_{corr}, but unless the geometry of a sample suite is held constant, such an observation could also reflect geometry changes. This is a significant issue on Mars, where the instrument sample geometry is not known and indeed changes from one sample to the next.

[16] Finally, GUAPX now offers the possibility to include a single invisible component such as H_2O+ in the matrix. In this case the given *H* value is used, and the concentration of the invisible component is determined as the difference between 100% and the summed visible oxide concentrations.

4. Total Oxide Concentration Results for GRMs by Fixed and Iterative Matrix Approaches

[17] Some useful initial insight can be gained by comparing the results of the fixed matrix approach and the iterative matrix approach for the total oxide concentrations in the GRMs. The suppliers' certificates provide recommended oxide concentrations for major and minor elements. The

Table 2. Total Oxide Concentrations With Related Data and Results[a]

GRM	Total Certificate Concentration of Visible MMO (wt %)	GUAPX Fixed Matrix Total MMO (wt %)	GUAPX Iterative Matrix H_{corr}[b]	R(Si) Fixed Matrix	Certificate Concentration of Invisible Components[c] (wt %)
			Group A		
BE-N (B)	96.51	100.0	1	1.033	2.98
BR (B)	96.63	98.9	1	1.033	3.16
PM-S (B)	98.91	98.7	1	0.984	0.92
WS-E (B)	98.27	102.0	1	1.05	1.42
AGV1 (A)	98.88	99.5	0.988	1.037	0.81
BCR1 (A)	99.21	100.5	1	1.03	0.78
DR-N (A)	97.48	98.2	0.973	1.014	2.32
AC-E (R)	99.22	98.3	0.977	0.985	0.29
GA (R)	98.79	101.1	1	1.004	0.98
GH (R)	99.21	102.8	1.02	1.02	0.76
GS-N (R)	98.63	99.0	0.978	1.013	1.2
MA-N (R)	96.37	94.2	93.8	0.951	2.26
AN-G (AN)	99.16	101.9	1	1.01	0.74
AL-I (M)	99.37	98.5	0.976	1.006	0.62
DT-N (M)	98.23	98.4	0.982	1.063	1.52
FK-N (M)	99.55	102.2	1	1.006	0.41
VS-N (G)	97.81	94.8	0.944	0.959	0
			Group B		
GL-O (M)	94.08	88.8	0.898	0.966	5.58
Mica-Fe (M)	95.61	91.2	0.925	0.975	3.36
Mica-Mg (M)	95.28	90.1	0.901	0.977	2.26
UB-N (M)	88.92	81.8	0.831	0.985	11.23
BX-N (O)	88.08	82.5	0.853	1.003	11.92
GXR1 (O)	92.89	91.7	0.942	0.937	4.37
			Group C		
Jsd2 (S)	96.58	101.5	1.03	1.02	3.22
MAG1 (S)	91.9	91.4	0.922	1.064	13.68

[a]In column 1 B, basalt; A, andesite; R, rhyolite; AN, anorthosite; M, mineral; S, sediment; O, other; G, glass. Column 2 gives the suppliers' total concentrations of major and minor oxides (MMO) in geochemical reference materials and column 3 our fixed matrix results. Column 4 shows the factor by which the geometric constant H was reduced to achieve 100% MMO in the iterative matrix approach. Column 5 gives the ratio of measured silicon concentration to the certificate value in the fixed matrix calibration. Column 6 gives the suppliers' concentrations of light "invisible" components.
[b]If the oxide total is within the range 99–101 wt %, GUAPX does not apply any correction and the table shows the value 1 for H_{corr}.
[c]H_2O+, CO_2, Li2O, etc.

APXS detects all these elements with the exception of boron, lithium and zirconium. Although barium L lines are sometimes detectable by the APXS, the detection limit is estimated to be ~2000 ppm (R. Gellert, private communication, 2009) and we therefore neglected it in the sum. The K X-rays of boron and lithium are not detectable, while the K X-rays of Zr in the sample have negligible intensity relative to the zirconium K X-rays that arise from fluorescence of the detector collimator by scattered plutonium L X-rays. For this iterative matrix work, we used the H value determined in Part I. The correction term $k(Z)$ remained at the value 1.0 for all elements, corresponding to the FM analysis reported in Part I.

[18] In the second column of Table 2, we give the total concentration from the suppliers' certificates for those oxides whose cations are detectable. Because GUAPX provides the total oxide concentration of all visible elements, the second column also contains trace oxides whose concentrations exceed 0.25%; neglect of the other trace elements is inconsequential to the present argument. The history of these GRMs as regards preheating to remove adsorbed water H_2O- is not fully known to us. Some were heated to ~110°C and stored in a dessicator, while some were not. All were placed in turn in the APXS analysis chamber and held under vacuum for several hours prior to analysis and during analysis: this would remove some or all of any superficial water that was still present. We assumed here that all H_2O- had been removed, and we normalized the certificate oxide totals to recognize this very small adjustment. In the third column we give our corresponding fixed matrix total oxide concentrations found in Part I, and in the fourth the H_{corr} values found in the present work by the iterative matrix approach. The R(Si) values from Part I are reprised in the fifth column: as noted before, their standard deviation of 3.3% is presumed to arise from statistical counting error and from small variations in the distance from the sample surface to the X-ray detector; a 0.5 mm variation in the ~30 mm distance would cause the observed effect. The suppliers' total concentrations of bound water and carbon dioxide (and in a very few cases, fluorine, elemental carbon and lithium oxide), which are "invisible" to the APXS, are quoted in the final column. Our first objective is to compare the summed visible oxide concentrations determined using the fixed matrix approach in Part I with the H_{corr} values found here using the iterative matrix approach. If, for example, a given GRM has an oxide total of 97% in the fixed matrix approach, one expects to find an H_{corr} value of 0.97 in the iterative matrix approach. Any other outcome would reveal problems with the iterative approach.

[19] We examine first those GRMs which can be characterized as nearly pure minerals or, via the TAS scheme of Part I, as basalts, andesites, rhyolites and anorthosite; data

Table 3. Ratio of Summed Visible Oxide Concentrations Between Fixed Matrix Solution Values and Suppliers' Certificate Values

Group	GRM Type	Ratio
A	Basalts	1.024
A	Andesites	1.009
A	Rhyolites	1.006
A	Minerals AL-I, DT-N, FK-N	1.007
B	Minerals GL-O, UB-N, Mica-Fe, Mica-Mg; Others	0.945

on these cases occupy the upper portion of Table 2 and they are denoted collectively as group A. The summed concentration, according to the suppliers, of the invisible components in group A ranges up to ~3 wt % (percentage of total weight). There is excellent consistency between the fixed matrix oxide totals and the iterative matrix H_{corr} values. We can then conclude for group A that no significant deterioration in accuracy of the visible oxide total is incurred by using the iterative approach as opposed to the fixed matrix approach.

[20] Next for group A, we compare our measured total oxide concentrations and the corresponding certificate values. On average, our measurement is 2.4% in excess for basalts, and the excess falls progressively through andesites to essentially zero for rhyolites and for the three minerals in group A. These ratios are collected in Table 3. We recollect from Part I and from section 2 above that our fixed matrix approach overestimated Na and Al concentrations in basalts. A semiquantitative explanation was given in terms of mineral phase inhomogeneity, and this effect can explain part of the excess.

[21] There are three cases in group A which merit extra attention. The values of both the fixed matrix concentration and the H_{corr} are lowest for MA-N and VS-N, albeit in good agreement with one another. The two R(Si) values are also low in the same ratio, which suggests that the cause in each case is simply sample placement error. For DT-N, R(Si) is a high outlier, but the oxide total is accurately determined; this does not appear to be a geometric issue, and perhaps sample phase heterogeneity is responsible.

[22] Matters are more complex for the six GRMs in group B, which is composed of the cases in which the certificate measurable oxide total is less then the 96–100% range seen in the upper part of Table 2. Most of these cases have significant H_2O+ and/or CO_2 content, and several have a heterogenous mineral phase structure. We continue to observe excellent agreement between the fixed matrix and iterative matrix modes, but if we compare our results to the certificate values, we find a different outcome as compared to group A. For five of the six cases (GXR1 is the exception) our approach fails to identify about 5% of the total oxide mass. Several potential causes for this may be considered. Four of the group B GRMs have large iron content. When one converts the measured iron concentration to FeO or Fe_2O_3, the difference in the bound oxygen concentration is a factor 1.11. GUAPX assumes only the FeO form when it makes this conversion. The oxygen thus neglected in any Fe_2O_3 component is presumably part of the deficit in the oxide sum. Applying the obvious correction moves the result in the required direction but is insufficient to provide agreement. Another possibility is that these GRMs have reabsorbed H_2O- while in storage. A third possibility is that the large normalization of the oxide sums in these cases might distort the individual element concentrations; this will be investigated in section 5.

[23] There are, unfortunately, only two sediments in group C, and here we are unable to draw any general conclusions. JSd-2, with its small bound water content, could easily fit within group A. On the other hand, MAG-1 has several atypical aspects, including a very high R(Si) value in the fixed matrix solution. In our work on deducing invisible element content from measured and predicted Rayleigh/Compton ratios [*Campbell et al.*, 2008], the MAG-1 result suggests that its invisible content is several percent less than that given in the supplier's certificate. This result is consistent with Table 3, where we see a discrepancy between the supplier's value of 13.7% and our estimate of about 8% for the unaccounted component. P. King (private communication, 2008) suggests that the preheating of MAG-1 may cause loss of organic carbonate, which would explain our results.

5. Element Concentration Results by Fixed and Iterative Matrix Approaches

[24] We can now shift attention from oxide totals to individual element concentrations, and check if there are any significant changes in the latter when we shift from the established fixed matrix approach of Part I to the iterative matrix approach of this paper. In Table 4 we show the results for five representative GRMs, four from group A and one from group B. The first three group A cases chosen are, in TAS terminology, a basalt (BR), an andesite (DR-N) and a rhyolite (AC-E); the fourth is a mineral (FK-N) which has a very low concentration of invisible components. For the group B representative we chose the phyllosilicate reference material UB-N, which has the largest invisible content in this group. The H value is the same as that used in the fixed matrix work of Part I. The quantity presented in Table 4 is the ratio of our determined concentrations between the iterative matrix mode and the fixed matrix mode.

[25] The GRMs of group A, which contain only small invisible component (H_2O+, CO_2, Li_2O) concentrations, show only small changes in R value. Indeed, these changes

Table 4. Ratio of R Value Between Iterative Matrix and Fixed Matrix Solutions for Major and Minor Elements With High Content of Invisible Components[a]

	Group A				Group B
GRM	FK-N	AC-E	DR-N	BR	UB-N
Certificate invisible (wt %)	0.41%	0.29%	2.32%	3.16%	11.2%
Na	0.997	1.017	1.008	0.996	
Mg			1.007	1.003	1.201
Al	0.993	1.014	1.005	0.992	1.192
Si	0.995	1.016	1.014	1.013	1.205
K	0.993	1.018	1.020	1.014	
Ca			1.013	1.007	1.23
Ti			1.029	1.021	
Mn			1.028	1.025	1.28
Fe	1.003	1.027	1.033	1.025	1.28
Zn		1.027	1.042	1.019	

[a]FK-N, pure mineral; AC-E, rhyolite; DR-N, andesite; BR, basalt; UB-N, mineral.

Table 5. Detailed Analysis of R Values for Sodium, Magnesium, Aluminum, and Phosphorus by the Fixed Matrix Approach[a]

	Quantity	Na	Mg	Al	P	Ti
All GRMs	R_{wm}	0.99 ± 0.02	0.90 ± 0.015	1.04 ± 0.01	1.23 ± 0.05	0.925 ± 0.02
All GRMs	R_m ± 2sd	1.06 ± 0.24	0.91 ± 0.24	1.05 ± 0.20	1.27 ± 0.52	0.94 ± 0.18
All GRMs	Range of R	1.05 ± 0.21	0.89 ± 0.23	1.03 ± 0.21	1.15 ± 0.41	0.99 ± 0.17
GRM Subgroups						
Basalts per TAS	R_{wm} ± EEM	1.21 ± 0.06	0.90 ± 0.02	1.20 ± 0.03	1.30 ± 0.05[b]	0.93 ± 0.02[b]
Andesites per TAS	R_{wm} ± EEM	1.04 ± 0.07	0.86 ± 0.06	1.07 ± 0.03	1.30 ± 0.05[b]	0.93 ± 0.02[b]
Rhyolites per TAS	R_{wm} ± EEM	0.965 ± 0.025	0.97 ± 0.11	1.06 ± 0.02	1.30 ± 0.05[b]	0.93 ± 0.02[b]
Minerals	R_{wm} ± EEM	0.96 ± 0.03	0.89 ± 0.02	0.99 ± 0.02	0.80 ± 0.12	0.96 ± 0.04
Pure elements and simple compounds	Range of R	0.88 ± 0.03	0.96 ± 0.03	1.01 ± 0.01	0.87 ± 0.02	0.99 ± 0.02

[a]The anomalous R-value for UB-N is excluded.
[b]Results are averaged across all basalts, andesites, and rhyolites, since no significant differences were observed among these rock types.

are within the accuracy estimates with which R was determined in the fixed matrix approach (Table 1). There is an indication, however, of a very small differential effect for the heavier element concentrations determined by XRF relative to the light element concentrations determined by PIXE. The concentrations of the elements manganese through zinc increase in the iterative mode by a slightly greater amount than those of the elements sodium through silicon. This differential effect is small in the materials having the smallest content of invisible components (FK-N and AC-E) and larger in the two cases that have 2–4% of invisible components (BR and DR-N). Some insight into this situation is provided by the results for UB-N with its 11.2 wt % of invisible H_2O+ and CO_2. Here the differential effect is again present, but is much larger and cannot be ignored as being comparable with experimental uncertainties.

[26] We ascribe this differential effect to the imposition of the 100% closure rule in the iterative matrix mode, i.e., the normalization of the oxide concentrations to 100 wt % total. We must recall that this correction is made on the basis of the visible components only, since in the iterative matrix mode we are regarding the GRM as an unknown sample and thus cannot take advantage of our a priori knowledge of the H_2O+ and CO_2 contents. In effect, in this mode, we are computing the matrix term with the invisible content replaced, erroneously, by an equal wt % of the visible matrix. This increases the average atomic number of the matrix and hence the attenuation of the excited X-rays within it. The attenuation increases more for the lighter elements and less for the heavier elements. We thus expect a differential effect which favors the heavier element concentrations, which is what is observed in our results. Similar effects are seen for the other GRMs of group B which carry significant invisible components.

[27] In sum, we see that the presence of undetectable light element components beyond the oxygen which is stoichiometrically bound to visible elements has the potential to cause errors in the APXS analysis using the iterative matrix mode. The fundamental parameters approach helps us to understand the causes and the trends of these errors.

6. Specially Tailored Calibration Schemes for Analysis of Different Sample Types

[28] We now address the task of defining the correction function $k(Z)$ in equation (1), with the objective of refining our iterative matrix approach. At first, we shall base the discussion on only the group A GRMs, for which the issue of the effect of invisible components on the closure rule is small. We defer consideration of the distorting effects of invisible components until the end of the section.

[29] There are six elements (sodium, magnesium, aluminum, phosphorus, chlorine and titanium) for which the work of Part I suggests that a correction factor needs to be introduced. The evidence for five of the six cases is summarized in Table 5, which is assembled from the results of Part I, and has been discussed in detail in section 2. From Table 5, one can extract the desired $k(Z)$ value as $R_X(Z)$, where X might denote the mean value of R, or the weighted mean R_{wm}, or the median R_{med} of the entire range of R values for the element in question. The mean is obviously biased toward those reference materials for which the most data points exist. At first glance, adoption of R_{wm} appears to be the most rigorous of these choices on statistical grounds, but two objections can be raised: the weighted mean is biased toward those GRMs that have the smallest error estimates; and this choice would necessarily assume that the data for any given Z constitute a valid sample of a single population. The latter assumption could be avoided by adopting the median of the data for each of these elements, with correspondingly rather large uncertainty limits derived from the range of R values. In this "range calibration," $k(Z)$ would be set equal to $R_{med}(Z)$.

[30] The evidence in Table 5 shows that for sodium, aluminum and phosphorus, different GRM types within group A as defined via the TAS scheme do indeed have clearly different R_{wm} values. In other words, there are subgroups within the overall group of GRMs, an observation which negates the assumption mentioned in the previous paragraph, and which suggests that for these particular elements it is not appropriate to adopt a single $k(Z)$ value across all the reference materials. If we now regard each of these GRM subgroups as a distinct population, we can assign to each a unique $k(Z)$ determined as its $R_{wm}(Z)$ value in that subgroup; the associated uncertainty is then rigorously equal to the fractional standard deviation of its mean. For sodium and aluminum, the pertinent subgroups are (1) basalts, (2) andesites, and (3) rhyolites and minerals. For phosphorus there are just two subgroups, namely, rocks and minerals. For titanium, we suggested above that the effect arises because this element is present in the accessory titanite phase, for which the matrix term computed on the assumption of homogeneity is inaccurate. For magnesium, we define a common $k(Z)$ value across all the GRMs, reflecting the belief that the issue in this case does not derive from the nature of the GRM. Chlorine is a less clear-cut case; in

Table 6. Comparison Between Concentrations in Five GRMs Determined by the Tailored Iterative Matrix Method Including Invisible Water and the Certificate Concentration Values

	Measured Concentration[a] (wt %)				
Z	BR	DR-N	AC-E	FK-N	UB-N
11	2.28 (2.28)	2.14 (2.23)	4.65 (4.88)	1.85 (1.92)	
12	8.22 (8.05)	2.73 (2.66)			21.41 (21.43)
13	5.40(5.43)	9.06 (9.3)	8.01 (7.82)	10.12 (9.87)	1.02 (1.55)
14	18.45 (17.95)	25.1 (24.78)	32.6 (33.05)	30.45 (30.45)	18.31 (18.61)
15	0.43 (0.46)	0.07 (0.11)			
16	0.027 (0.039)	0.038 (0.035)			0.051 (0.02)
17	0.033 (0.035)	0.04 (0.04)	0.023 (0.018)		0.082 (0.08)
19	1.12 (1.17)	1.37 (1.42)	3.78 (3.75)	11.02 (10.66)	
20	10.28 (9.92)	5.21 (5.05)	0.28 (0.244)		0.575 (0.87)
22	1.60 (1.57)	0.68 (0.66)	0.066 (0.066)		
24	0.037 (0.038)				0.245 (0.232)
25	1.61 (1.55)	0.177 (0.171)	0.039 (0.045)		0.104 (0.094)
26	8.83 (9.06)	6.75 (6.81)	1.75 (1.78)	0.059 (0.061)	5.82 (5.89)
28	0.030 (0.026)				0.2 (0.2)
30	0.016 (0.016)	0.017 (0.015)	0.022 (~0)		0.009 (0.009)
INV	2.2 (3.2)	2.4 (2.32)	1.4 (0.29)	0 (0.41)	14.1 (11.2)

[a]Certificate concentrations are in parentheses.

thirteen GRMs which include all the different rock types in the overall suite, chlorine occurs at concentrations less than 0.1% and has $R_{wm} = 1.19 \pm 0.08$. In contrast, the ocean sediment MAG-1 has 3 wt % chlorine and R = 0.86, a value that is compatible with the neglect of the detector ICC layer. We therefore adopted a $k(Z)$ value of 1.19 with the proviso that we would only apply it in situations of very low chlorine concentration.

[31] The scheme thus developed will be referred to as a "tailored calibration," because it is tailored to deal with issues that are specific to and different in the various types of GRM presently under discussion. A final question is whether this tailored, iterative matrix approach can give any indication of the presence of invisible components. This can be addressed by use of an additional feature of GUAPX which has not yet been mentioned or exploited. In addition to allowing the incorporation of invisible oxygen which is stoichiometrically coupled to the cations, GUAPX also permits the definition of one independent invisible component (e.g., H_2O+) which makes up the difference between the visible oxide sum and 100 wt %. This invisible component plays a full role in the computation of matrix effects such as ion deceleration and X-ray attenuation, and GUAPX provides its concentration along with that of the various elements present.

7. Tests and Pitfalls of Different Calibration Schemes Within the Iterative Matrix Approach

[32] Four different tests were undertaken to ascertain the accuracy of the approaches outlined in the previous section. As with all the work described here, they employ MER calibration data recorded by *Gellert et al.* [2006].

7.1. Representative GRMs as Unknowns

[33] Our first objective here is to test the tailored version of the iterative matrix approach. We successively removed five representative GRMs from the calibration suite and regarded each as an unknown sample. This sample set, introduced in section 5, comprised one basalt (BR), one andesite (DR-N), one rhyolite (AC-E), one mineral with negligible invisible content (FK-N), and one mineral with very large invisible content (UB-N). It was thus necessary to redefine the $k(Z)$ values in each case such that the earlier fixed matrix results (see Part I) for these cases played no role in determining $k(Z)$ for their subgroup. In each analysis, bound water was included in our treatment as an independent invisible component. The results are in Table 6. The agreement between the element concentrations obtained by this approach and the suppliers' recommended elemental concentrations is excellent. An exploration of uncertainties in the measured quantities will not be pursued here, since associated error estimates were detailed in Part I. It is evident that the tailored calibration scheme works well, but of course its use is predicated on having a priori knowledge that enables us to assign a given sample to a rock group for which the appropriate $k(Z)$ values have been predetermined.

[34] Another point of interest here is the results for invisible H_2O+. In cases where the H_2O+ concentration is small (1–3 wt %), there is an indication of its presence, but this at the level of the overall uncertainty in the total oxide concentration. In the one case where it is large, there is a remarkably good agreement between our determination and the certificate value. In the five cases examined, the invisible components are H_2O+ and CO_2, the former dominating. It should be noted, though, that only one invisible component can be accommodated in GUAPX, and we have assumed it to be H_2O+. It is useful to assess in the UB-N case what errors would have arisen in the elemental analysis if the tailored solution had been used but the invisible component ignored. The results are in Table 7. Omission of the invisible component H_2O+ causes significant error in the element concentrations, while inclusion gives excellent agreement of these concentrations with the certificate values. This supports our suggestion in section 4 that additional adsorbed water may be present in this sample. The demonstrated influence of inclusion versus exclusion of water on the element concentrations in the phyllosilicate reference material UB-N, together with the very accurate results for element con-

Table 7. Element Concentrations for UB-N[a]

Z	TIM (wt %)	TIM+H_2O (wt %)	Certificate (wt %)
12	24.12	21.42	21.43
13	1.21	1.02	1.55
14	21.64	18.31	18.61
16	0.06	0.05	0.02
17	0.12	0.08	0.08
20	0.67	0.57	0.87
24	0.30	0.24	0.23
25	0.13	0.10	0.09
26	7.36	5.82	5.89
28	0.27	0.20	0.20
30	0.012	0.009	0.009

[a]The first column is from the tailored iterative matrix solution (TIM), with invisible H_2O+ ignored, the second is from that solution with invisible H_2O+ included (TIM+H_2O), and the third is the certificate value for this GRM.

centrations in the former case, have clear implications for the analysis of such materials on Mars.

7.2. Sediments

[35] Only two sediments were included in the suite of GRMs used by *Gellert et al.* [2006], namely, the stream sediment JSd-2 and the ocean floor material MAG-1. These are regarded as unknowns for the purposes of this section. Because of the lack of a priori knowledge regarding their mineral composition, we refrained from introducing $k(Z)$ corrections for sodium, aluminum, phosphorus and chlorine, and restricted such corrections to magnesium and titanium. The results are in Table 8, along with results for other GRMs which will be discussed in section 7.3. Our concentrations for the lightest elements show errors of up to 20%, a conclusion which was already evident in Part I. This is not surprising, given that it is not possible to assign these materials to some well-defined rock group and thus tailor the calibration. It does point to the need to be conservative in assigning uncertainties in APXS analysis of sediments, and to the need to incorporate a considerably larger number of such reference materials (especially sediments) in future APXS calibration exercises. As a final note, the 7.5 wt % concentration found for H_2O+ in MAG-1 changes only slightly if CO_2 is substituted as the invisible component in the sediments. The supplier's certificate gives the total concentration of H_2O+ and CO_2 as 13.7%. Our result suggests, as does our argument in section 4, that much of the CO_2 was removed in the preheating of this sample to remove H_2O-. This observation provides a note of caution as regards the use of sediment reference materials.

7.3. Issue of Mineral Phase Heterogeneity: Trachytes and Anorthosite

[36] *Gellert et al.* [2006] included the anorthosite reference material AN-G in their calibration suite; this GRM cannot be assigned to the basalt, andesite, rhyolite or mineral subgroups. They also included the two trachyte reference materials ISH-G and MDO-G in their calibration exercise. We chose in Part I not to use these trachytes in our fixed matrix calibration, as the supplier provided only provisional element concentrations and no information concerning H_2O+. Here we shall regard them as completely unknown samples. These three cases have mineralogies which enable us to reinforce the mineral phase argument which we developed earlier as a possible explanation for the low results for sodium and aluminum concentrations in basalts and andesites. This in turn helps us to illustrate the degree of error that may be incurred in APXS analysis where there is no a priori indication of the mineralogy.

[37] Because these cases do not fall within the rock classifications (basalt, andesite, rhyolite) in which we have developed and tested tailoring schemes for sodium and aluminum, no $k(Z)$ corrections were employed for these two elements. We retained the $k(Z)$ correction for magnesium, where we believe that a database issue is the most likely cause. We also retained the corrections for P, Cl and Ti, on the grounds that the low concentrations observed here indicate that these elements exist in accessory phases. The results are in Table 8.

[38] For the two trachytes, in contrast to basalts and andesites treated in the same manner, the aluminum concentrations from GUAPX are in excellent agreement with the suppliers' values. We take this to reflect the fact that aluminum resides in the sanidine phase, which is the majority

Table 8. Measured Element Concentrations for Sediments, Trachytes, and Anorthosite[a]

Element	MAG-1 (wt %)	JSd-2 (wt %)	ISH-G (wt %)	MDO-G (wt %)	AN-G (wt %)
Na	2.24 (2.76)	1.96 (1.82)	3.45 (3.84)	3.65 (3.97)	1.31 (1.21)
Mg	2.04 (1.75)	1.92 (1.66)	0.43 (0.79)	0.64 (1.25)	1.11 (1.09)
Al	9.03 (8.4)	7.41 (6.57)	9.87 (9.92)	9.79 (9.77)	16.0 (15.81)
Si	24.7 (22.8)	29.1 (28.6)	26.9 (27.3)	26.77 (26.6)	21.74(21.69)
P			0.09 (0.14)	0.05 (0.07)	
S	0.33 (0.38)	0.90 (1.29)			
Cl	2.63 (3.0)		0.08 (nd)		0.02 (0.03)
K	3.11 (2.86)	0.92 (0.96)	5.33 (5.43)	3.71 (3.53)	0 (0.11)
Ca	1.05 (0.98)	2.62 (2.64)	2.24 (2.52)	2.81 (3.35)	11.92(11.39)
Ti	0.43 (0.44)	0.50 (0.37)	0.35(0.48)	0.75 (0.96)	0.12 (0.13)
Mn	0.087 (0.074)	0.099 (0.094)	0.09(0.09)	0.059(0.062)	0.044 (0.031)
Fe	5.18 (4.67)	7.66 (7.88)	2.79(3.45)	3.17 (4.35)	2.35 (2.36)
Cu		0.11 (0.11)			
Zn	0.015 (0.013)	0.19 (0.21)	0.006 (0.007)	0.004 (0.007)	
Br	0.026 (0.024)				
Sr			0.027 (0.035)	0.070 (0.073)	
W		0.010 (0.010)			
H_2O+	7.50 (13.7)	0 (3.2)	4.3 (?)	4.2 (?)	0 (0.74)

[a]Certificate concentrations are in parentheses.

Table 9. Measured Element and H_2O+ Concentrations for Meteorite Samples[a]

Element	Zagami (wt %)	Murchison (wt %)	Murchison With H_2O+ (wt %)
Na	1.00 (0.97)	0.28 (0.17)	0.25
Mg	6.33 (6.17)	12.46 (12.44)	11.11
Al	3.40 (3.03)	1.22 (1.21)	1.08
Si	23.3 (23.8)	14.55 (13.59)	12.86
P	0.36 (0.36)	(0.10)	
S	0.13	3.03 (3.07)	2.60
Cl	0.016	0.036 (0.02)	0.03
K	0 (0.08)	(0.03)	
Ca	7.64 (8.03)	1.34 (1.31)	1.24
Ti	0.56 (0.58)	(0.08)	
Cr	0.22 (0.23)	0.39 (0.3)	0.34
Mn	0.44 (0.40)	0.23 (0.16)	0.19
Fe	14.27 (13.80)	25.86 (21.24)	21.85
Ni		1.57 (1.3)	1.27
Cu	0.015	0.017 (0.014)	0.014
Zn	0.007	0.025 (0.02)	0.02
H_2O+	0	Omitted	12.7 (11–15.6[b])

[a]Concentrations in brackets are from the Max Planck Institüt fur Chemie, Mainz, Germany.

[b]First number in brackets is H_2O+; second is sum of H_2O+ and CO_2 assuming all carbon present in form of CO_2.

mineral phase in trachytes. The excellent potassium result also reflects that it occurs predominantly in the sanidine. Our calcium result is low by 10–16 wt %, and we attribute this to its presence in the minority plagioclase phase. While sodium is present in both these phases, its result (low by about 10%) suggests that a significant portion of the sodium is in the minority phase. Magnesium and iron show very large discrepancies (48% and 23%, respectively) which presumably reflect their residence in the accessory phases biotite and pyroxene.

[39] The matrix terms in our X-ray yield equations and the matrix corrections in the method of *Gellert et al.* [2006] represent the "average" rock matrix (averaged over all mineral phases) and are therefore dominated by the majority mineral phase. It follows that if an element happens to reside in a minority or accessory phase, these corrections will be inaccurate, the more so in the latter. For basalts, we argued in Part I that sodium and aluminum reside in minority feldspar and thus the matrix term, based largely on the majority pyroxene, olivine etc, is inappropriate for these elements. Calculations supported this argument in semi-quantitative fashion, showing that our concentration results for sodium and aluminum would be expected to fall low while those for magnesium would be reliable; this is precisely the outcome that we had observed. Now for trachytes, we observe even larger effects; it is the calcium, iron and, most dramatically, the magnesium results which fall low, which we attribute to their being hosted mainly by minority and accessory phases. The ~4 wt % bound water suggested by GUAPX for the trachytes seems unrealistically high. It is presumably a consequence of the underestimate of the concentrations of Fe, Ca, Mg and Ti coupled to the 100% closure requirement. It follows that the extraction of bound water concentrations by our method needs to be approached with great caution.

[40] The majority mineral in the anorthosite GRM AN-G is plagioclase feldspar, dominated by aluminum, silicon and calcium, and so the matrix corrections are accurate for these three elements. Agreement of the concentrations is satisfactory in these cases, and also for sodium, which is a minor component of this phase. The excellent agreement for magnesium, presumably present in the minority mafic phase, is somewhat surprising.

[41] These examples support our previous suggestion that in situ rock analysis by the APXS is subject to significant errors for elements which are hosted by minority mineral phases and very large errors when elements are hosted by accessory phases. For the moment, the only way to alleviate this situation is to use other evidence to identify the specific rock type and to develop tailored calibration schemes for different rock types based on an enlarged and diversified group of GRMs. When a rock is composed predominantly of a single mineral phase, good results can be expected for the elements that comprise that phase; this is seen in the results of Table 7 for the iron-magnesium silicate reference material UB-N.

7.4. Meteorite Samples

[42] The suite of calibration materials used by *Gellert et al.* [2006] included a fine-grained and homogenous sample from the Martian meteorite Zagami, which had been analyzed at the Max Planck Institüt (MPI) by conventional methods (R.G. Rieder, private communication, 2003). The composition of shergottite generally resembles that of terrestrial basalt [*Lodders*, 1998], and so analyzing it with the tailored approach developed above for basalts as defined in Figure 1 provides a useful test of our calibration scheme. The suite also included an MPI sample of the Murchison meteorite, which has significant bound water content, and so it appeared to be a second useful candidate for analysis. The results for these two samples are in Table 9.

[43] For the Zagami meteorite sample, the element concentration results show excellent agreement with the MPI values. The one significant exception is aluminum, for which our concentration lies 10% high relative to the MPI value. This may reflect that the observed aluminum resides in the minority plagioclase. The overall outcome supports our tailored approach for calibration and measurement of basalts.

[44] For the Murchison sample, we show results from analyses with and without the inclusion of invisible H_2O+. The first analysis tells us that invisible components are present, since the oxide sum is only about 92%. The second indicates that if all the invisible components are H_2O+, then its contribution is 12.7%. The MPI concentrations for invisible components are 1.7% carbon and 9.3% H_2O+. Taking the carbon to be elemental, we would have a minimum invisible component of 11.0%; taking all the carbon to be in the form CO_2 would give a maximum 15.5%. Our result falls within this range. It might be noted that this sample was subjected to preheating [*Rieder et al.*, 2003] to ensure a dry surface for alpha particle backscattering measurements. We see again that a fully calibrated APXS is able to provide a useful estimate of water and CO_2 content. Of course, it has to be reiterated that GUAPX cannot deal separately with two independent invisible components.

8. Conclusions

[45] In Part I of this work, we showed that the MER APXS could be calibrated and its geometric constant *H*

determined by a fixed matrix solution of the equation relating X-ray yield to concentration via fundamental physics parameters and detector properties. This was done using existing APXS spectra of geochemical reference materials. Necessary corrections $k(Z)$ to this "constant" were of two types: incomplete knowledge of detector properties (specifically the ICC layer) led to corrections for elements whose X-rays had very small penetration into the X-ray detector, and in certain igneous rock types where specific elements resided in minority phases an empirical correction was necessary. The latter corrections allow us to "tailor" our calibration for a few specific igneous rock types defined by use of a TAS diagram. Basalts require the most dramatic tailoring of the calibration, while rhyolites require no rock-specific tailoring. In contrast to the prior calibration method of *Gellert et al.* [2006], which did not differentiate among rock types, the present approach does account for mineralogical differences, albeit empirically, and for a limited set of rock and mineral groups.

[46] In this paper, we have developed an iterative matrix approach to spectrum processing that is suitable for unknown samples. It rests on the determination of a geometric constant and the corrections to this constant based both on instrumental issues and on mineralogy, derived from the fixed matrix approach mentioned above. However, the need to invoke the 100% closure rule on the total oxides present in an unknown sample, common to both our approach and that of *Gellert et al.* [2006], leads to errors in the determined concentrations when "invisible" components such as H_2O+ and CO_2 are present. We augmented our approach with the ability to include one such independent, invisible component, subject to the restriction that the concentrations of all components sum to 100 wt %. The invisible component is treated rigorously in the matrix correction procedure.

[47] To test our tailored calibration scheme, we took five GRMs from Gellert's suite representing each of the typical rock types contained within it (basalt, andesite, rhyolite, mineral) and treated them as "unknowns." In the mineral case, we chose one "dry" mineral and one water-bearing mineral to test our treatment of invisible elements. In Part I, we had derived empirical tailoring corrections for the four defined groups. For magnesium, the applied correction reflected instrumental issues, while for sodium, aluminum, chlorine, phosphorus and titanium, we had argued that they arose mainly from mineral phase heterogeneity. Our "tailored" iterative matrix approach gave excellent results both for element concentrations and that of H_2O+. This was the outcome even in a case such as the phyllosilicate UB-N which contains 11.2% of bound water and CO_2. Further support for both these conclusions was found in analyses of samples of the meteorites Zagami and Murchison. Our element concentrations for the Zagami sample, which resembles terrestrial basalt, agreed well with values determined by conventional methods for the same sample. For the Murchison sample, our result for the invisible component content fell within the range that is suggested by published values of H_2O+ and carbon content.

[48] To further probe the effects of mineral phase heterogeneity, we subjected one anorthosite and two trachytes from Gellert'suite to our iterative matrix analysis approach. The results for several major and minor elements show consistently that the approach is accurate if these elements are present in a majority phase. But if they are in a minority phase, the matrix terms in our equations are not accurate for these elements, and their concentrations can depart by up to 20% from the expected values. For elements present in accessory phases, the errors can reach as high as 50%. This phase heterogeneity issue is not unique to our analysis method: it is intrinsic to any X-ray emission method but the short range of the helium ions in the APXS setup renders light elements particularly vulnerable. *Gellert et al.* [2006] were clearly aware of these issues in general. By determining their "weighting" and "response" parameters through a best fit over a large suite of GRMs of different type, they went some way toward accommodating these effects. But in such an approach the resulting parameters will reflect the particular mineralogical makeup of the selected GRMs; a different suite biased toward different rock types could give different parameters. The present work probes much more extensively into the specifics of these effects as a function of rock type, and provides a quantitative caution as regards the uncertainties of light element analysis in rocks and soils by the APXS. It should be stressed that these effects are to be expected; they are the reason why in terrestrial analysis of rocks by X-ray fluorescence, the samples are first fused to a homogenous glass.

[49] Several guidelines for future APXS calibration and use can be drawn. In the calibration with GRMs, the fixed matrix approach is to be preferred since it avoids invoking 100% closure and it treats invisible components rigorously. If an iterative matrix approach is used which invokes closure, GRMs containing a significant concentration (>~3%) of invisible components should be avoided; otherwise accuracy will be compromised. However, GUAPX does provide a way around this by permitting inclusion of one independent invisible component. These are important points if water-bearing sediment standards are to be included in the calibration. Next, a tailored iterative matrix approach offers more accurate analysis than a nontailored one, provided there is other evidence on hand to assist in identifying the mineralogy of a sample such that the most appropriate calibration scheme can be applied.

[50] It follows from this work that if constant sample APXS geometry could be maintained (in other words, a fixed sample instrument distance and a smooth sample surface), our iterative matrix approach could be used to determine water content of samples. Of course, on Mars, natural surfaces can be textured and rough even after abrasion. Moreover, on the current MER mission, the sample instrument distance varies from one sample to the next and there is no means of accurately determining the distance from sample to instrument in each case. This then necessitates recourse to the 100% closure rule for every sample. In turn, this means that analyses will be inaccurate if mineralogically bound water or carbonate is present. There is considerable evidence for the presence of bound water in the white subsurface material known as the Paso Robles soil discovered by the Spirit rover. The APXS shows that it has high levels of iron and sulfur [*Brückner et al.*, 2008] and the Mossbauer spectrometer shows that ~80% of the iron is in the ferric state [*Morris and Klingelhöfer*, 2008]; these observations suggest the presence of ferric sulfate and hence, possibly, hydration. Photography shows color consistent with this interpretation [*Wang et al.*, 2008]. Various hydrated sulfates

have been suggested as candidates [*Lane et al.*, 2008]. We recently introduced a new analysis method [*Campbell et al.*, 2008] that employs the X-ray scatter peaks in the APXS spectra, and it suggests the presence of water in these materials. It follows from all this evidence for hydration of the Paso Robles material that the existing elemental analysis, which ignores bound water, is only a first-order approximation. For these reasons, we shall attempt to link our two methods for determination of hydration, in the interests of achieving a consistent set of results for both elemental and water concentrations in the Paso Robles materials. In retrospect, however, had the MER APXS devices been equipped with an independent means of measuring source-device distance, application of our present method which combines 100% closure with the presence of independent invisible components might have afforded a direct determination of the level of hydration. This finding appears highly relevant to design of future APXS models.

[51] The next phase of this work will transfer the fixed matrix calibration to the APXS instruments on the Spirit and Opportunity rovers, and will conduct iterative matrix analyses of a subset of the extensive MER sample suite. Given the predominance of basalts in the samples analyzed by the Spirit rover, the success of the tailored iterative matrix calibration for basalts is a promising prelude to a reanalysis of these data. The good results for the Zagami Martian meteorite support this statement. At the same time, calibration of the MSL APXS is proceeding under the direction of R. Gellert, with a GRM suite that is greatly expanded both in number and in variety of rock type relative to that of the MER mission. There will be a much greater emphasis on sediment GRMs in this work, relative to the MER calibration where only two sediment GRMs were used. These data will provide us with an opportunity to test and refine the concepts and approaches developed here.

[52] **Acknowledgments.** This work was supported by the Natural Science and Engineering Research Council of Canada and by the Canadian Space Agency. The authors are indebted to Ralf Gellert for many illuminating discussions.

References

Brückner, J., G. Dreibus, R. Gellert, S. Squyres, H. Wänke, A. Yen, and J. Zipfel (2008), Mars Exploration Rovers: Chemical composition by the APXS, in *The Martian Surface*, edited by J. Bell, pp. 58–101, Cambridge Univ. Press, New York.

Campbell, J. L., D. Higuchi, J. A. Maxwell, and W. J. Teesdale (1993), Quantitative PIXE micro-analysis of thick specimens, *Nucl. Instrum. Methods Phys. Res., Sect. B*, *77*, 95–109, doi:10.1016/0168-583X(93)95530-I.

Campbell, J. L., G. Cauchon, M.-C. Lépy, L. McDonald, J. Plagnard, P. Stemmler, W. J. Teesdale, and G. White (1998), A quantitative explanation of low-energy tailing features of Si(Li) and Ge X-ray detectors using synchrotron radiation, *Nucl. Instrum. Methods Phys. Res., Sect. A*, *418*, 394–404, doi:10.1016/S0168-9002(98)00889-4.

Campbell, J. L., R. Gellert, M. Lee, C. L. Mallett, J. A. Maxwell, and J. M. O'Meara (2008), Quantitative in situ determination of hydration of bright high-sulfate Martisan soils, *J. Geophys. Res.*, *113*, E06S11, doi:10.1029/2007JE002959.

Campbell, J. L., M. Lee, B. N. Jones, S. M. Andrushenko, N. G. Holmes, J. A. Maxwell, and S. M. Taylor (2009), A fundamental parameters approach to calibration of the Mars Exploration Rover Alpha Particle X-ray Spectrometer, *J. Geophys. Res.*, *114*, E04006, doi:10.1029/2008JE003272.

Eggert, T., O. Boslau, J. Kemmer, A. Pahlke, and F. Wiest (2006), The spectral response of silicon X-ray detectors, *Nucl. Instrum. Methods Phys. Res., Sect. A*, *568*, 1–11, doi:10.1016/j.nima.2006.07.011.

Gellert, R., et al. (2006), Alpha Particle X-ray Spectrometer (APXS): Results from Gusev crater and calibration report, *J. Geophys. Res.*, *111*, E02S05, doi:10.1029/2005JE002555.

Lane, M. D., J. L. Bishop, M. D. Dyar, P. L. King, M. Parente, and B. C. Hyde (2008), Mineralogy of the Paso Robles soils, *Am. Mineral.*, *93*, 728–739, doi:10.2138/am.2008.2757.

LeMaitre, R. W., et al. (2002), *Igneous Rocks: A Classification and Glossary of Terms, Recommendations of the International Union of Geological Sciences, Sub-commission of the Systematics of Igneous Rocks*, Cambridge Univ. Press, Cambridge, U. K.

Lodders, K. (1998), A survey of shergottite, nakhlite and chassigny meteorites whole-rock compositions, *Meteorit. Planet. Sci.*, *33*, A183–A190.

Morris, R. V., and G. Klingelhöfer (2008), Iron mineralogy and aqueous alteration on Mars from the MER Mössbauer spectrometers, in *The Martian Surface*, edited by J. Bell, pp. 339–365, Cambridge Univ. Press, New York.

Potts, P. J. (1987), *A Handbook of Silicate Rock Analysis*, Blackie, Glasgow, U. K.

Rieder, R. G., R. Gellert, J. Brückner, G. Klingelhöfer, G. Dreibus, A. Yen, and S. W. Squyres (2003), The new Athena Alpha Particle X-ray Spectrometer for the Mars Exploration Rovers, *J. Geophys. Res.*, *108*(E12), 8066, doi:10.1029/2003JE002150.

Wang, A., et al. (2008), Light-toned salty soils and coexisting Si-rich species discovered by the Mars Exploration Rover Spirit in Columbia Hills, *J. Geophys. Res.*, *113*, E12S40, doi:10.1029/2008JE003126.

S. M. Andrushenko, J. L. Campbell, J. A. Maxwell, and S. M. Taylor, Guelph-Waterloo Physics Institute, University of Guelph, Guelph, ON N1G 2W1, Canada.